



## Gas–liquid countercurrent integration process for continuous biodiesel production using a microporous solid base KF/CaO as catalyst

Shengyang Hu<sup>1</sup>, Libai Wen<sup>1</sup>, Yun Wang, Xinsheng Zheng, Heyou Han<sup>\*</sup>

State Key Laboratory of Agricultural Microbiology, College of Science, Huazhong Agricultural University, Wuhan 430070, China

### HIGHLIGHTS

- ▶ A novel continuous flow integration process was developed for biodiesel production.
- ▶ The process has the characteristic of countercurrent contact reaction between gas and liquid.
- ▶ The process has the characteristic of rapid and automatic separation for glycerol on line.
- ▶ The process has the characteristic of cyclic utilization of methanol.
- ▶ Biodiesel yield of as high as 93.7% was obtained in this integration process.

### ARTICLE INFO

#### Article history:

Received 24 November 2011  
Received in revised form 29 April 2012  
Accepted 22 May 2012  
Available online 9 July 2012

#### Keywords:

Biodiesel  
Gas–liquid countercurrent integration process  
Microporous catalyst  
Transesterification

### ABSTRACT

A continuous-flow integration process was developed for biodiesel production using rapeseed oil as feed-stock, based on the countercurrent contact reaction between gas and liquid, separation of glycerol on-line and cyclic utilization of methanol. Orthogonal experimental design and response surface methodology were adopted to optimize technological parameters. A second-order polynomial model for the biodiesel yield was established and validated experimentally. The high determination coefficient ( $R^2 = 98.98\%$ ) and the low probability value ( $Pr < 0.0001$ ) proved that the model matched the experimental data, and had a high predictive ability. The optimal technological parameters were: 81.5 °C reaction temperature, 51.7 cm fill height of catalyst KF/CaO and 105.98 kPa system pressure. Under these conditions, the average yield of triplicate experiments was 93.7%, indicating the continuous-flow process has good potential in the manufacture of biodiesel.

© 2012 Elsevier Ltd. All rights reserved.

### 1. Introduction

Biodiesel is a biodegradable, nontoxic, environmentally beneficial fuel and it possesses excellent emission characteristics (Jon Van, 2005). Currently, biodiesel is produced mainly by transesterification of triglyceride with alcohols, such as methanol or ethanol, in the presence of base (Rashid et al., 2008) or acid (Aranda et al., 2008; Di Serio et al., 2005) catalysts. Common processes for biodiesel production are one-step or two-step batch transesterification processes. As opposed to the continuous processes, batch processes has several drawbacks (Darnoko and Cheryan, 2000): (1) requirement for larger reactor volumes, thus higher capital investments; (2) lower efficiency due to start-up and shut-down characteristics; (3) batch-to-batch variations in the quality of the products; (4) higher labor costs. Therefore, the aim of this study was to create

a continuous flow process as a potential solution to reduce manufacturing costs.

Another possible way to reduce cost is the application of solid catalysts especially solid nano-catalysts rather than homogenous catalysts because of heterogeneous catalysts have a higher catalytic activity, are easier to separate and reuse, allow for simpler operational procedures, and generate less pollution (Akbar et al., 2009; Feng et al., 2010; Gao et al., 2009; Granados et al., 2007; Hu et al., 2011; Verziu et al., 2008; Wen et al., 2010a; Xu et al., 2009). CaO is an active and promising heterogeneous catalyst for the production of biodiesel (Granados et al., 2009; Kouzu et al., 2008; Liu et al., 2008; Kawashima et al., 2008; Kawashima et al., 2009; Veljković et al., 2009; Viriya-empikul et al., 2010). Previously, a KF/CaO solid catalyst was investigated in the transesterification of tallow oil with methanol (Wen et al., 2010b) in batch experiments, and it was shown that the catalyst had excellent catalytic properties. In the present study, a continuous-flow integration process was utilized for producing biodiesel from rapeseed oil using microporous KF/CaO as solid catalyst. Parameters such as reaction temperature, fill height of the catalyst and system

<sup>\*</sup> Corresponding author. Tel./fax: +86 02787288246.

E-mail address: [Hyhan@mail.hzau.edu.cn](mailto:Hyhan@mail.hzau.edu.cn) (H. Han).

<sup>1</sup> These authors equally contributed to this work.

pressure were optimized with an orthogonal experimental design and response surface methodology (RSM).

## 2. Methods

### 2.1. Catalyst preparation and characterization

The catalyst was prepared by the impregnation method (Wen et al., 2010b). Briefly, 100 g of CaO powder was immersed in 150–200 mL aqueous solution with 25 g KF for 1 h, and dried at 105 °C for 2 h, followed by 3 h calcination in a muffle furnace at 600 °C. The catalyst was stored in a desiccator. The surface structure of the catalyst was characterized with JEM-100SX transmission electron microscopy (TEM) and JEOLJSM-6390 scanning electron microscope (SEM), respectively. X-ray diffraction (XRD) measurements were performed on a Rigaku D/Max-III A powder X-ray diffractometer using Cu/K $\alpha$  radiation, over a  $2\theta$  range of 10–70° with a step of 0.02 at a scanning speed of 10 deg min<sup>-1</sup>. The phases were identified using the powder diffraction file (PDF) database (JCPDS, International Centre for Diffraction Data (Sun et al., 2010)). Pore size was analyzed with an Autosorb-1 pore size analyzer using N<sub>2</sub> adsorption–desorption with a measuring range of 0.1–3500 m<sup>2</sup> g<sup>-1</sup> specific area and 2–200 nm pore diameter. The repeatability error was within 2%. The basic strength (H<sup>-</sup>) was determined based on the color change of Hammet indicators (Watkins et al., 2004). Basicity was analyzed according to Zhu et al. (1999). Briefly, 0.05 g solid base catalyst was shaken for 5 min in 0.02 mol L<sup>-1</sup> aqueous HCl (5 ml), and the remaining acid was titrated with 0.02 mol L<sup>-1</sup> aqueous NaOH. The Hammet indicators used in this study were: phenolphthalein (9.3), 2,4-dinitroaniline (15.0) and 4-nitroaniline (18.4). The numbers in parentheses are their pK<sub>a</sub> values.

### 2.2. Process design

Since the contact area of gas–liquid is larger than that of liquid–liquid, theoretically, a higher production efficiency can be obtained through gas–liquid contact. Scheme 1 shows a diagram of a continuous-flow process which mainly contains three fluidic modules in series (signed as FM01, FM02 and FM03) and one rectification column. Each fluidic module consists of three zones, upper, middle and lower zone, which are designated as Z1, Z2 and Z3, separately. The upper zone is a condenser for methanol vapor. The middle zone is a reactor which contains the microporous solid base catalyst. The lower zone is a separator to separate glycerol and biodiesel on-line. Heating of the middle and the lower zones is provided by a thermostatically controlled water bath capable of maintaining the temperature within  $\pm 0.2$  °C, and the temperature of each zone is controlled separately by two temperature controllers. To form a continuous flow system, two high pressure pumps were used to link the three fluidic modules. The transesterification reaction was carried out in a glass reactor (in Z2 of each fluidic module) with 6 cm in outer diameter and 65 cm in length. The reactor was filled with 5-mm glass beads (ca. 2 cm height) and solid base catalyst.

The process operated by adding methanol through a flow indicator and controller (FIC) into separator (length Z3 of FM01, 6 cm o.d.  $\times$  65 cm). The methanol was vaporized in Z3 and the vapor phase entered the reactor (Z2 of FM01) from the bottom of reactor. Rapeseed oil was injected into the reactor (Z2 of FM01) filled with methanol vapor moving in the countercurrent flow direction. This approach allowed direct contact between both phases with a large contact area on the surface of solid base catalyst, promoting heat and mass transfer. After transesterification, the mixture flowed into separator (Z3 of FM01) and automatically formed two phases, crude biodiesel (upper layer) and glycerol (lower layer). The glycerol was

separated on-line moved into storage. The crude biodiesel from FM01 was pumped to FM02 for further reaction with methanol.

In order to increase the reaction rate, a high methanol/oil molar ratio was allowed in the continuous flow process. The methanol vapors entering from the bottom of the reactor agitated the reaction mixture and accelerated the reaction rate and improved the efficiency of transesterification. The excess methanol can be automatically reused in the independent fluidic module in Scheme 1.

### 2.3. Transesterification and production analysis

In the continuous flow process, the flow rate of rapeseed oil (acid value <1 mg KOH g<sup>-1</sup> and moisture <1%) and methanol were 18 mL min<sup>-1</sup> and 16–20 mL min<sup>-1</sup>, separately. The total fill height was in the range of 30–60 cm (ca. 90–180 g), including catalyst and glass beads (ca. 2 cm height). The separator temperature was maintained at 90 °C and the reactor temperature was varied in the range of 70–90 °C. The separator was pressurized with N<sub>2</sub> in the range of 104.65–105.98 kPa. The average daily throughput of biodiesel and glycerol were 23 kg and 2.1 kg, respectively.

The biodiesel was quantitative analyzed in the presence of methyl salicylate as internal standard by GC using a HITACHI163 gas chromatography instrument. The oven temperature ramp program was 190 °C for 2 min, 190–280 °C at 10 °C min<sup>-1</sup>, and holding for 6 min at 280 °C. The injector and detector temperatures were 300 °C and the flow rate of N<sub>2</sub>, H<sub>2</sub> and air were 25, 40 and 400 mL min<sup>-1</sup>, respectively. The split ratio was 30:1. The mass concentration of biodiesel was obtained by GC analysis and the yield of biodiesel was calculated by the following equation:

$$\text{Yield} = \frac{m_{\text{actual}}}{m_{\text{theoretical}}} \approx \frac{C_{\text{esters}} \times n \times V_{\text{esters}}}{m_{\text{oil}}} \times 100\%$$

$$\approx \frac{C_{\text{esters}} \times n \times V_{\text{oil}}}{m_{\text{oil}}} \times 100\% \approx \frac{C_{\text{esters}} \times n}{\rho_{\text{oil}}} \times 100\%$$

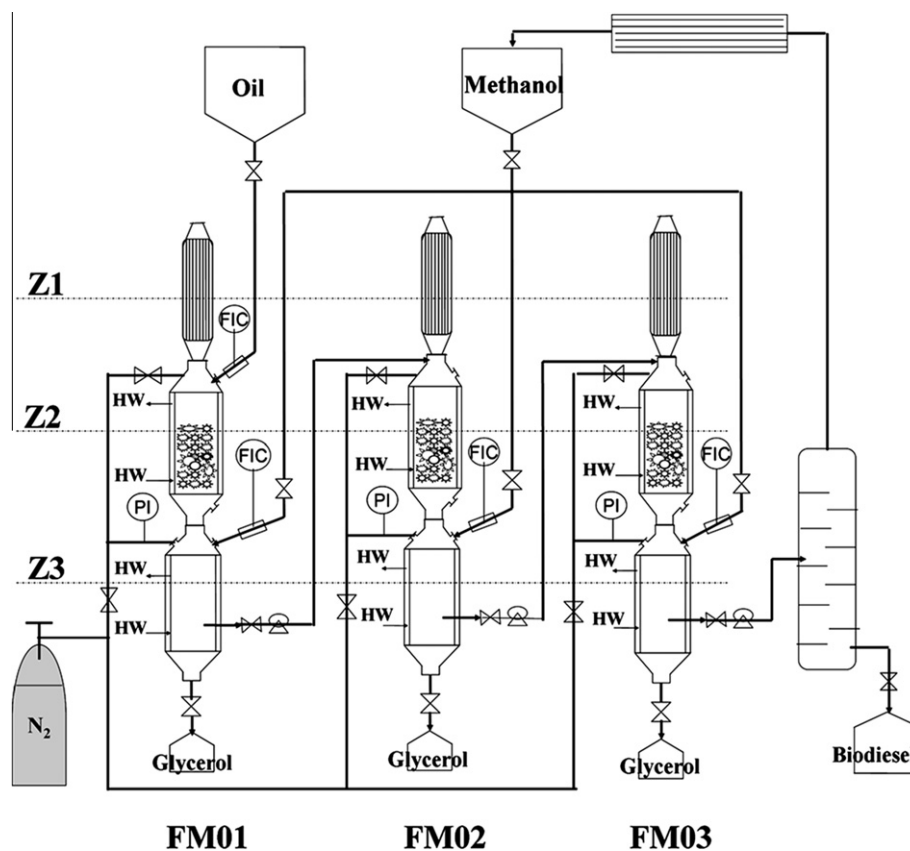
where both  $m_{\text{actual}}$  (g) and  $m_{\text{theoretical}}$  (g) are the actual mass and theoretical mass of biodiesel;  $m_{\text{oil}}$  (g) is the mass of rapeseed oil;  $n$  is the diluted multiple of biodiesel;  $C_{\text{esters}}$  (g mL<sup>-1</sup>) is the mass concentration of biodiesel;  $\rho_{\text{oil}}$  (g mL<sup>-1</sup>) is the density of rapeseed oil;  $V_{\text{esters}}$  (mL) and  $V_{\text{oil}}$  (mL) are the volumes of biodiesel and rapeseed oil, respectively (He et al., 2007).

### 2.4. Statistical analysis

Some independent factors would bring significant effect on biodiesel yield in the transesterification reaction. Therefore, according to the yield of biodiesel, orthogonal experiment was designed to pick out the significant factors, and the central composite design was further adopted to optimize the experimental condition. The central composite design was made of 12 experiments with four factorial points, four central points and four axial points. The independent factors and their levels in coded and actual values are shown in Table 1. The distance of the axial points encoded  $+\alpha$  and  $-\alpha$  from the center point was  $\alpha = 2^{n/4}$ , where  $n$  is the number of independent variables. The experimental matrix for the central composite design is summarized in Table 2. All experiments are conducted in a random order. Experimental data is analyzed with software SAS version 8.1 (SAS Institute Inc., Cary, NC, USA). The association between dependent and independent variables in present study is explained by the following second-order polynomial model:

$$Y = \beta_0 + \beta_1 X_1 + \beta_2 X_2 + \beta_3 X_1^2 + \beta_4 X_1 X_2 + \beta_5 X_2^2 \quad (1)$$

where  $Y$  is the dependent variable (biodiesel yield);  $X_1$  and  $X_2$  are the independent variables;  $\beta_0$ ,  $\beta_1$ ,  $\beta_2$ ,  $\beta_3$ ,  $\beta_4$  and  $\beta_5$  are intercept, linear, quadratic and interaction constant coefficients, respectively.



Scheme 1.

**Table 1**  
Levels of factors for the central composite design.

Levels	Factors	
	Reaction temperature ( $T/^\circ\text{C}$ )	Fill height of catalyst ( $H/\text{cm}$ )
$+\alpha$	87.1	57.1
+1	85	55
0	80	50
-1	75	45
$-\alpha$	72.9	42.9

**Table 2**  
Experimental matrix and experimental results for the central composite design.

Run	$X_T$	$X_H$	Y (%)
1	-1	-1	58.4
2	-1	+1	82.9
3	+1	-1	85.5
4	+1	+1	90.4
5	0	0	92.5
6	0	0	92.0
7	0	0	91.7
8	0	0	92.2
9	$+\alpha$	0	89.2
10	0	$+\alpha$	90.8
11	0	$-\alpha$	70.9
12	$-\alpha$	0	60.6

$X_T$ : coded value of reaction temperature.

$X_H$ : coded value of fill height of catalyst.

Y: biodiesel yield.

## 2.5. Fuel property determination

The main fuel properties of biodiesel included cetane number, density, kinematic viscosity, flash point, acid value and sulfur

content, acid value, ash content and water content. The properties were tested according to the methods in Table 3.

## 3. Results and discussion

### 3.1. Catalyst characterization

XRD imaging demonstrated that  $\text{KCaF}_3$  was produced during the impregnation stage (Wen et al., 2010b). Since impregnation releases heat, the temperature may reach  $120^\circ\text{C}$ . New crystal structure of  $\text{KCaF}_3$  can form under low temperature with the peak intensity increasing from room temperature to  $400^\circ\text{C}$  and decreasing from  $400$  to  $600^\circ\text{C}$ . With increasing temperatures, the  $\text{Ca}(\text{OH})_2$  diffraction peak diminished while a  $\text{CaO}$  diffraction peak formed. The peak of  $\text{CaO}$  started to form at  $400^\circ\text{C}$  while the peak of  $\text{Ca}(\text{OH})_2$  completely disappeared at  $600^\circ\text{C}$ . The  $2\theta$  angles ( $^\circ$ ) of  $\text{CaO}$  were  $32.12^\circ$ ,  $37.28^\circ$ ,  $53.80^\circ$ ,  $64.12^\circ$ ,  $67.34^\circ$ , while for  $\text{KCaF}_3$  they were  $28.74^\circ$ ,  $41.22^\circ$ ,  $51.26^\circ$ ,  $59.52^\circ$ , and  $18.02^\circ$ ,  $34.08^\circ$ ,  $47.14^\circ$ ,  $50.82^\circ$ ,  $54.36^\circ$ ,  $62.60^\circ$  for  $\text{Ca}(\text{OH})_2$ . Thus, the optimum calcinations temperature was  $600^\circ\text{C}$ , which was identical with the orthogonal test results (see Supplementary Table S1). The introduction of  $\text{KF}$  leads to the formation of  $\text{KCaF}_3$ , which enhanced catalytic activity and improved saponification resistance (Wang et al., 2009).

Images of the micro- and macro-structures of the catalyst are available in Supplementary Fig. S1. The catalyst is granular and porous with evenly distributed granules and abundant large pores. The granules are made up of several smaller granules  $30\text{--}100\text{ nm}$  in diameter which forms a porous structure. A honeycomb-like structure was observed on the surface of the catalyst. These results demonstrate that the catalyst has porous structure which increases the contact area between the catalyst and the substrates, further improving its catalytic ability and reaction efficiency.

**Table 3**  
Fuel properties of biodiesel sample with comparison to standards.

Test property	EN 14212	ASTM D6751	Biodiesel sample	Test method
Cetane number (min)	51	47	52	GB/386
Kinematic viscosity (mm <sup>2</sup> /s; 40 °C)	3.5–5.0	1.9–6.0	4.6	GB/T265
Flash point (°C)	120	130	>100	GB/T261
Pour point (°C)	–	–	–	GB/T510
Acid value (mg KOH g <sup>-1</sup> )	0.5max	0.8max	0.36	GB/T264
Sulfur content (mg kg <sup>-1</sup> )	10max	15max	1.4	GB/T387
Water content (mg kg <sup>-1</sup> )	500max	500max	traces	GB/T260
Ash content (mg kg <sup>-1</sup> )	24max	–	2	GB/T508

–: Not specified.

The nitrogen adsorption–desorption isotherms of the catalyst are given in Fig. 1a. The catalyst has a porous structure with a surface area of 109 m<sup>2</sup> g<sup>-1</sup>. The pore size distribution curve shows that the average pore size was 97 nm (Fig. 1b), which is consistent with the SEM and TEM observations. The high specific area and large pore were the major reason for high catalytic activity of KF/CaO. The basic strength (H<sup>-</sup>) of KF/CaO catalyst was in the range of 15.0–18.4 and the basicity of catalyst is 0.94 mmol g<sup>-1</sup> cat, indicating KF/CaO is a strong basic solid base catalyst.

### 3.2. Kinetic approach

The rate law for transesterification can be expressed as:

$$-r_0 = \kappa C_{\text{cat}0}^{\alpha} \cdot C_{\text{RO}0}^{\beta} \cdot C_{\text{Me}0}^{\gamma} \quad (2)$$

$r_0$  represents the initial reaction rate;  $\kappa$  is the reaction rate constant;  $\alpha$ ,  $\beta$  and  $\gamma$  represent the reaction orders, respectively;  $C_{\text{cat}0}$ ,  $C_{\text{RO}0}$  and  $C_{\text{Me}0}$  are the initial catalyst, rapeseed oil and methanol

concentrations, respectively. The concentration ratio of methanol to oil can be regarded as a parameter affecting the transesterification rate. Therefore, the rate law model also can be written as:

$$-r_0 = \kappa C_{\text{cat}0}^{\alpha} \cdot C_{\text{Me-RO}0}^{\beta} \quad (3)$$

The reaction temperature was held constant (70 °C). The reaction orders in this rate model were obtained by varying one reactant concentration while keeping the other reactant concentration constant.  $C_{\text{cat}0}$  and  $C_{\text{Me-RO}0}$  were 2–6 wt.% and 3–15, respectively. When the initial concentration of one reactant was changed, the value of  $r_0$  had a direct ratio correlation to the logarithmic value of the initial concentration of this reactant, and the proportional coefficient was the reaction order of this reactant. The apparent reaction orders for catalyst ( $\alpha = 2.09$ ) and concentration ratio of methanol to oil ( $\beta = 0.56$ ) were calculated from the slopes of the fitted straight lines in Fig. 2a and b. The correlations for the fitted lines were 0.99.

The activation energies ( $E_a$ ) were estimated from the Arrhenius plots. The  $E_a$  for the conversion of rapeseed oil to biodiesel using KF/CaO as catalyst was 17.30 kJ mol<sup>-1</sup> and the correlation coefficient ( $R$ ) was 0.98 (Fig. 3).

### 3.3. Continuous flow production of biodiesel

#### 3.3.1. Orthogonal experiment for determination of significant variables

That the analysis showed that reaction temperature has the greatest effect on biodiesel yield, followed by the fill height of solid base catalyst. The biodiesel yield reached a maximum value of 87.7% at 80 °C, probably due to the fact that liquid methanol turn into vapor with the elevation of reaction temperature above 80 °C (This is the boiling point under pressure) and the amount of methanol is decreased in the reaction system. Because the reaction is reversible, a decrease in the amount of methanol is not favorable for shifting the equilibrium to the product side. Therefore, the reaction temperature of 80 °C was adopted in our experiment. The yields of biodiesel were 78.8%, to 79.4%, and 86.4% for catalyst fill heights of 30, 40, and 50 cm, respectively (Table 4). A higher fill height decreased production efficiency (Table 4). Thus, the appropriate fill height of catalyst was 50 cm. The trend for system pressure on the biodiesel yield was similar to that of fill height of catalyst. The highest yield (82.5%) was observed at 105.98 kPa (Table 4).

Overall, the optimal combination of reaction temperature, fill height of catalyst and system pressure is 80 °C, 50 cm and 105.98 kPa, respectively.

#### 3.3.2. RSM

The experimental results corresponding to the central composite design are also shown in Table 2. The RSREG procedure from SAS is employed to fit the polynomial Eq. (1) to the experimental data. The coefficients of the full regression model equation are (in terms of coded factors):

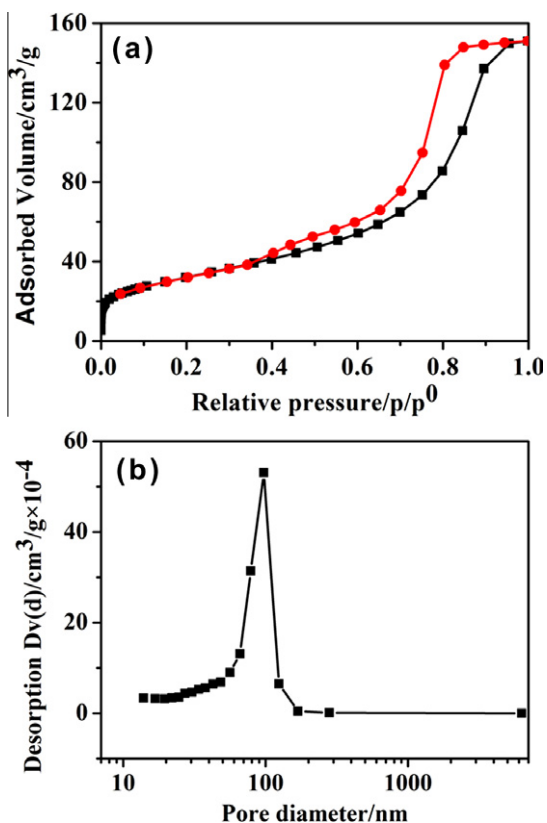


**Fig. 1.** Nitrogen adsorption–desorption isotherms (a) and pore size distribution curve (b) of the KF/CaO catalyst.

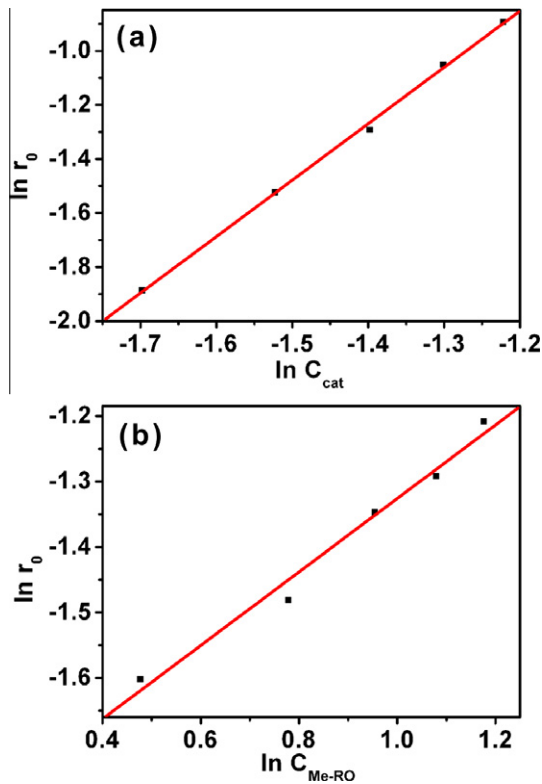


Fig. 2. Effect of reactant concentration on initial reaction rate: (a) catalyst ( $C_{cat}$ ); (b) concentration ratio of methanol to rapeseed oil ( $C_{Me-RO}$ ).

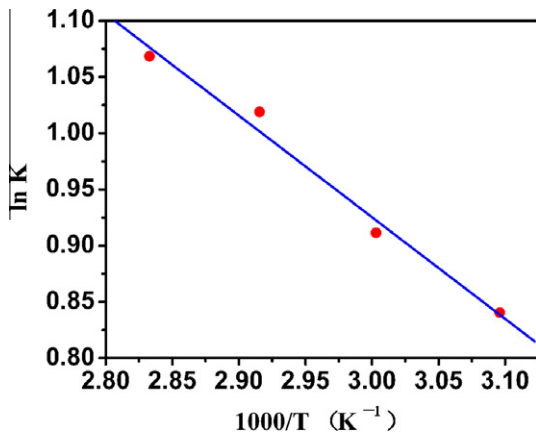


Fig. 3. Arrhenius plots for the conversion of rapeseed oil to biodiesel using KF/CaO catalyst. Temperature range: 50–80 °C.

$$Y (\%) = 92.10 + 9.38X_T + 7.19X_H - 8.25X_T^2 - 5.27X_H^2 - 4.90X_TX_H \quad (4)$$

where  $Y$  is the dependent variable (biodiesel yield);  $X_T$  and  $X_H$  are the reaction temperature and fill height of catalyst, respectively. From Eq. (4), positive coefficients for all linear terms indicate positive effects on the increase in biodiesel yield, while all the quadratic and interaction terms have negative effects. The fitted model was analyzed using analysis of variance ( $P$ -test) and the results of statistical analysis are summarized in Table 5. A very low  $P$ -value ( $<0.0001$ ) and a very high determination coefficient ( $R^2 = 98.98\%$ ) of the model indicate that the second-order polynomial regression model is highly significant and able to represent the actual relationship between the response and their variables.

Table 4  
Orthogonal analysis of technological parameters.

Run	Factors			Biodiesel yield (%)		
	$T$ (°C)	$P$ (kPa)	$H$ (cm)	FM 1	FM 2	FM 3
1	70	104.65	30	30.7	45.2	52.7
2	70	105.32	40	42.5	50.4	60.8
3	70	105.98	50	50.5	60.1	82.5
4	80	104.65	50	64.2	74.4	89.5
5	80	105.32	30	60.4	76.8	81.2
6	80	105.98	40	65.5	78.7	92.5
7	90	104.65	40	52.0	62.2	85.0
8	90	105.32	50	67.5	75.0	87.2
9	90	105.98	30	55.0	60.5	72.5
$K_1$	65.3	75.7	78.8			
$K_2$	87.7	76.4	79.4			
$K_3$	81.6	82.5	86.4			
$r$	22.4	6.8	7.6			

$K_1$ ,  $K_2$  and  $K_3$  are the average value of biodiesel yield at level 1, level 2 and level 3, respectively.  $r$  is pole difference of average value of biodiesel yield. FM1, FM2, FM3 are the biodiesel yield in fluidic module1, fluidic module2 and fluidic module3, respectively.  $T$ : reaction temperature;  $P$ : system pressure;  $H$ : fill height of catalyst.

The effects of reaction temperature and fill height of catalyst on biodiesel yield can be better evaluated using the response surface plot (Fig. 4) generated from the predicted model (Eq. (4)), where reaction temperature and fill height of catalyst are at the central point, i.e. 80 °C and 50 cm, respectively. As shown in Fig. 4, both variables have a positive effect on the biodiesel yield. However, their interaction was a negative effect on the biodiesel. The optimum parameters calculated through the polynomial regression model (Eq. (4)) were 81.5 °C and 51.7 cm for the reaction temperature and fill height of catalyst, respectively. Under the above optimal conditions, triplicate experiments were conducted to validate the precision of the polynomial regression model. The average value of biodiesel yield was 93.7%, which is in close agreement to the predicted value i.e. 95.8%. Therefore, this model is considered to be an accurate and reliable tool for predicting the biodiesel yield in continuous flow process.

### 3.4. Fuel properties of biodiesel

The test results are also summarized in Table 3 together with the relevant specifications from biodiesel standards of the European EN 14214 and the American ASTM D 6751. As illustrated in Table 3, the test results of biodiesel sample are close to, or the above, biodiesel standards.

### 3.5. Economic feasibility study

The solid base catalyst can be used continuously for more than 144 h and the biodiesel did not have to be washed with water. Therefore, the process causes almost no environmental pollution during production. Due to the characteristics of automatic

Table 5  
Analysis of variance for the fitted second-order polynomial regression model.

Source	DF	Sum of squares	$F$ value	$Pr > F$
Linear	2	1117.89	376.74	<0.0001
Quadratic	2	522.28	176.02	<0.0001
Cross-product	1	96.04	64.73	0.0002
Total model	5	1736.21	234.05	<0.0001
Lack of fit	3	8.56	25.18	0.0125
Pure error	3	0.34		
Total error	6	8.90		
$R^2 = 98.98\%$				

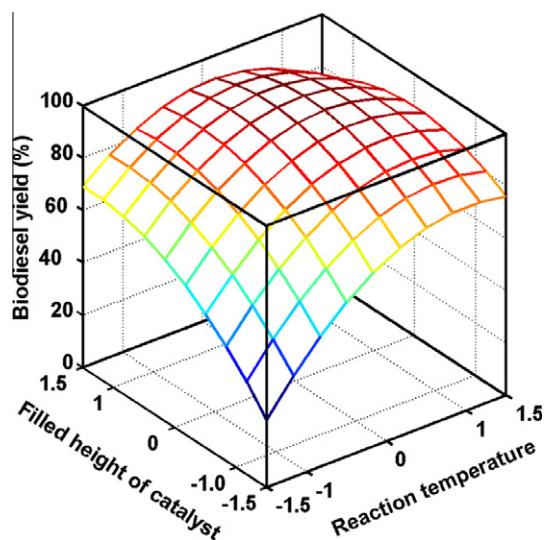


**Fig. 4.** Response surface plot of the second-order polynomial model for biodiesel yield as a function of reaction temperature and fill height of catalyst.

separation of glycerol on-line and cyclic utilization of methanol, the recovery of glycerin is ca. 90% and the methanol steam does not escape from the system. In one production cycle (144 h), the average throughput of biodiesel and glycerol are ca.138 and ca.12.6 kg, respectively and requires ca.145 kg of feedstock oil, 13.5 kg of methanol and 0.45 kg of catalyst. Since the market price of rapeseed oil is ca. 5500 ¥/ton in China (¥ is the Chinese currency, 6.3 ¥  $\approx$  1\$ in 2012), the total production cost including operating cost is ca. 884 ¥. The price of glycerol and biodiesel is ca.8000 ¥/ton and 6000 ¥/ton in China, respectively and therefore, total income of sale is ca. 928 ¥ including biodiesel and glycerol. The average profits would be ca.319 ¥/ton biodiesel.

The solid base catalyst KF/CaO can be reused for 16 times with no apparent loss of activity in batch process (Wen et al., 2010b). And the deactivated catalyst can be regenerated just by simple calcinations in air. The catalyst KF/CaO is inexpensive. In one continuous-flow production cycle (144 h), the catalyst cost is ca. 18 ¥. It is only 2% of total production cost. KF/CaO can contribute to decreasing the cost of biodiesel production due to its long catalyst lifetime and good stability.

The largest portion of manufacturing cost of biodiesel is attributed to the feedstock cost. With large-scale production of biodiesel, unit cost of biodiesel will be further reduced. Therefore, the continuous-flow production process using solid catalyst has obvious economic feasibility.

#### 4. Conclusions

A continuous-flow integration process was developed and successfully utilized for biodiesel production from rapeseed oil. A biodiesel yield of 95.8% was expected from the theoretically model and experimental determination gave 93.7% with less than 5% error; an indication of the adequacy of the model used. In addition, to biodiesel production, the novel continuous flow process should find application in a wide range of other important organic reactions using granular solid catalysts.

#### Acknowledgements

The authors gratefully acknowledge the support for this research by National Natural Science Foundation of China

(20975042, 21175051), the Fundamental Research Funds for the Central Universities (2010PY009, 2011PY139).

#### Appendix A. Supplementary data

Supplementary data associated with this article can be found, in the online version, at <http://dx.doi.org/10.1016/j.biortech.2012.05.143>.

#### References

- Akbar, E., Binitha, N., Yaakob, Z., Kamarudin, S.K., Salimon, J., 2009. Preparation of Na doped SiO<sub>2</sub> solid catalysts by the sol-gel method for the production of biodiesel from jatropha oil. *Green Chem.* 11, 1862–1866.
- Aranda, D., Santos, R., Tapanes, N., Ramos, A., Antunes, O., 2008. Acid-catalyzed homogeneous esterification reaction for biodiesel production from palm fatty acids. *Catal. Lett.* 122, 20–25.
- Darnoko, D., Cheryan, M., 2000. Continuous production of palm methyl esters. *J. Am. Oil Chem. Soc.* 77, 1269–1272.
- Di Serio, M., Tesser, R., Dimiccoli, M., Cammarota, F., Nastasi, M., Santacesaria, E., 2005. Synthesis of biodiesel via homogeneous Lewis acid catalyst. *J. Mol. Catal. A: Chem.* 239, 111–115.
- Feng, Y., He, B., Cao, Y., Li, J., Liu, M., Yan, F., Liang, X., 2010. Biodiesel production using cation-exchange resin as heterogeneous catalyst. *Bioresour. Technol.* 101, 1518–1521.
- Gao, L., Teng, G., Lv, J., Xiao, G., 2009. Biodiesel synthesis catalyzed by the KF/Ca–Mg–Al hydrotalcite base catalyst. *Energy Fuel* 24, 646–651.
- Granados, M.L., Alonso, D.M., Sádaba, I., Mariscal, R., Ocoń, P., 2009. Leaching and homogeneous contribution in liquid phase reaction catalysed by solids: The case of triglycerides methanolysis using CaO. *Appl. Catal. B: Environ.* 89, 265–272.
- Granados, M.L., Poves, M.D.Z., Alonso, D.M., Mariscal, R., Galisteo, F.C., Moreno-Tost, R., Santamaría, J., Fierro, J.L.G., 2007. Biodiesel from sunflower oil by using activated calcium oxide. *Appl. Catal. B: Environ.* 73, 317–326.
- He, H., Wang, T., Zhu, S., 2007. Continuous production of biodiesel fuel from vegetable oil using supercritical methanol process. *Fuel* 86, 442–447.
- Hu, S., Guan, Y., Wang, Y., Han, H., 2011. Nano-magnetic catalyst KF/CaO–Fe<sub>3</sub>O<sub>4</sub> for biodiesel production. *Appl. Energy* 88, 2685–2690.
- Jon Van, G., 2005. Biodiesel processing and production. *Fuel Process. Technol.* 86, 1097–1107.
- Kawashima, A., Matsubara, K., Honda, K., 2008. Development of heterogeneous base catalysts for biodiesel production. *Bioresour. Technol.* 99, 3439–3443.
- Kawashima, A., Matsubara, K., Honda, K., 2009. Acceleration of catalytic activity of calcium oxide for biodiesel production. *Bioresour. Technol.* 100, 696–700.
- Kouzu, M., Kasuno, T., Tajika, M., Yamanaka, S., Hidaka, J., 2008. Active phase of calcium oxide used as solid base catalyst for transesterification of soybean oil with refluxing methanol. *Appl. Catal. A: Gen.* 334, 357–365.
- Liu, X., He, H., Wang, Y., Zhu, S., Piao, X., 2008. Transesterification of soybean oil to biodiesel using CaO as a solid base catalyst. *Fuel* 87, 216–221.
- Rashid, U., Anwar, F., Moser, B.R., Ashraf, S., 2008. Production of sunflower oil methyl esters by optimized alkali-catalyzed methanolysis. *Biomass Bioenergy* 32, 1202–1205.
- Sun, H., Ding, Y., Duan, J., Zhang, Q., Wang, Z., Lou, H., Zheng, X., 2010. Transesterification of sunflower oil to biodiesel on ZrO<sub>2</sub> supported La<sub>2</sub>O<sub>3</sub> catalyst. *Bioresour. Technol.* 101, 953–958.
- Veljković, V.B., Stamenković, O.S., Todorović, Z.B., Lazić, M.L., Skala, D.U., 2009. Kinetics of sunflower oil methanolysis catalyzed by calcium oxide. *Fuel* 88, 1554–1562.
- Verziu, M., Cojocaru, B., Hu, J., Richards, R., Ciuculescu, C., Filip, P., Parvulescu, V.I., 2008. Sunflower and rapeseed oil transesterification to biodiesel over different nanocrystalline MgO catalysts. *Green Chem.* 10, 373–381.
- Viriya-empikul, N., Krasae, P., Puttasawat, B., Yoosuk, B., Chollacoop, N., Faungnawakij, K., 2010. Waste shells of mollusk and egg as biodiesel production catalysts. *Bioresour. Technol.* 101, 3765–3767.
- Wang, Y., Hu, S.-y., Guan, Y.-p., Wen, L.-b., Han, H.-y., 2009. Preparation of mesoporous nanosized KF/CaO–MgO catalyst and its application for biodiesel production by transesterification. *Catal. Lett.* 131, 574–578.
- Watkins, R.S., Lee, A.F., Wilson, K., 2004. Li–CaO catalysed tri-glyceride transesterification for biodiesel applications. *Green Chem.* 6, 335–340.
- Wen, G., Yan, Z., Smith, M., Zhang, P., Wen, B., 2010a. Kalsilite based heterogeneous catalyst for biodiesel production. *Fuel* 89, 2163–2165.
- Wen, L., Wang, Y., Lu, D., Hu, S., Han, H., 2010b. Preparation of KF/CaO nanocatalyst and its application in biodiesel production from Chinese tallow seed oil. *Fuel* 89, 2267–2271.
- Xu, L., Wang, Y., Yang, X., Hu, J., Li, W., Guo, Y., 2009. Simultaneous esterification and transesterification of soybean oil with methanol catalyzed by mesoporous Ta<sub>2</sub>O<sub>5</sub>/SiO<sub>2</sub>–[H3PW12O40/R] (R = Me or Ph) hybrid catalysts. *Green Chem.* 11, 314–317.
- Zhu, J., Chun, Y., Wang, Y., Xu, Q., 1999. Attempts to create new shape-selective solid strong base catalysts. *Catal. Today* 51, 103–111.